2011-12

Photoexpansion and photobleaching effects in oxysulfide thin films of the GeS2+Ga2O3 system

Physica B, Amsterdam : Elsevier BV, v. 406, n. 23, p. 4381-4386, Dec. 2011
http://www.producao.usp.br/handle/BDPI/50034

Physica B 406 (2011) 4381–4386

Contents lists available at SciVerse ScienceDirect

Physica B

journal homepage: www.elsevier.com/locate/physb

Photoexpansion and photobleaching effects in oxysulfide thin films of the $GeS_2+Ga_2O_3$ system

A.C. Mendes [a,*], L.J.Q. Maia [b,c], S.H. Messaddeq [c], Y. Messaddeq [c], S.J.L. Ribeiro [c], M. Siu Li [a]

[a] Instituto de Física de São Carlos, Universidade de São Paulo, C.P. 369, CEP 13566-590, São Carlos, SP, Brazil
[b] Instituto de Física, Universidade Federal de Goiás, C.P. 131, CEP 74001-970, Goiânia, GO, Brazil
[c] Instituto de Química, UNESP Araraquara, C.P. 355, CEP 14801-970, Araraquara, SP, Brazil

ARTICLE INFO

Article history:
Received 16 June 2011
Received in revised form
17 August 2011
Accepted 29 August 2011
Available online 5 September 2011

Keywords:
Oxysulfide
Optical bandgap
Photoexpansion
Photobleaching
Thin films

ABSTRACT

Oxysulfide systems undergo structural transformations upon illumination with laser light of near bandgap energy, as well as chalcogenide materials (glasses and films). In this paper, photoinduced effects such as photoexpansion and photobleaching were observed in $GeS_2+Ga_2O_3$ (GGSO) films synthesized by electron beam evaporation. A surface expansion of the thin films and a shift to shorter wavelengths of the optical absorption edge were observed as a result of UV laser irradiation (wavelength of 351 nm) and they are dependent on laser power density, exposure time and film composition. These parameters were varied to evaluate and enhance the observed effects. In addition, the irradiated GGSO samples exhibited a decrease in refractive index, measured with a prism-coupling technique, which makes these films suitable candidates for applications as gratings and waveguides in integrated optics.

1. Introduction

An extensive research has been made on materials for optical recording because the density of information storage in optical media can be up to two orders of magnitude higher than in magnetic disks. Some kinds of films have potential in this area and have been investigated as optical recording media for mass-memory applications [1,2]. In these applications, the basic mechanism used to record information is generally photoinduced effect, a subject that has been broadly investigated for more than 30 years, but not completely understood [3]. It seems that the photoinduced changes appear universally in covalent chalcogenide glasses such as GeS_2 [4], $Ge_{35}S_{65}$ [5], $Ge_{25}Ga_{10}S_{65}$ [6], As_2S_3 [7], $As_{36}Se_{64}$ [8], and in oxide compounds, such as GeO_2 [9]. However, it is interesting to explore mixtures of oxysulfide glasses that are more resistant to atmospheric attack and combine high optical non-linearity with moderate photosensitivity [10].

Oxysulfide systems, like GeO_2-GeS_2 glasses, undergo a variety of optical and structural changes as a result of illumination with near-bandgap energy [11,12]. A redshift (photodarkening) or blueshift (photobleaching) of the optical absorption edge [13] and volume changes [14] upon light illumination are examples of photoinduced phenomena, which can be used to fabricate diffractive, waveguide and fiber structures in these materials [15,16]. More attention has been given to the problem of oxygen-assisted photoinduced phenomena in Ge–S films. Tanaka et al. [5] were the first one to observe that the photobleaching of a $Ge_{35}S_{65}$ film depends on the air pressure. A modification with gallium was used to improve the glass stability of germanium sulfide glasses and recent results about $Ge_{25}Ga_{10}S_{65}$ (GGS) glasses [17] showed the presence of oxygen in their surface due to environmental exposure, even though this element was not present during glass preparation.

In this paper, we report a study on the photoinduced effects observed in $GeS_2+Ga_2O_3$ (GGSO) glass films. The 90 GeS_2+10 Ga_2O_3 (mol%) composition was selected because of its stability and, in terms of atomic percentage ($Ge_{28}Ga_6S_{56}O_9$), this glass system can be compared to the previously studied (GGS glasses) and provides fundamental insights into the presence of oxygen in photoinduced effects on the film samples. Previous structural study of photoinduced changes in this kind of films has shown that these phenomena are a consequence of the Ge–S bonds break down and the formation of new Ge–O bonds, with an increase of the modes associated to Ge–O–Ge bonds and mixed oxysulfide tetrahedral units (S–Ge–O) [18]. In order to evaluate the importance of oxygen in photoinduced phenomena, photoexpansion and photobleaching effects were observed when the samples were exposed to UV radiation. Optical absorption, refractive index and profile-meter measurements were performed.

* Corresponding author. Tel.: +55 16 33738085; fax: +55 16 33738085.
E-mail address: alecarlausp@yahoo.com.br (A.C. Mendes).

0921-4526/$ - see front matter © 2011 Elsevier B.V. All rights reserved.
doi:10.1016/j.physb.2011.08.091

2. Materials and methods

2.1. Film deposition

Oxysulfide glass ingots (90% GeS_2 + 10% Ga_2O_3) were prepared by melting and quenching method using crystalline powders with 99.9999% of purity (GeS_2, Ga_2O_3 and S). The precursor compounds were sealed in a quartz ampoule, evacuated up to 10^{-3} Pa, melted at 900°C during 6h and then quenched in water. Film specimens of different thickness and composition were deposited by electron beam evaporation from the crushed ingots with an electron beam voltage of 7 KV and an evaporation rate of 1 $Å s^{-1}$ in a vacuum of 10^{-6} Pa onto borosilicate substrates (known as B270 substrate) held at room temperature.

Three samples of the deposited films were selected: film A (0.36 μm-thickness), film B (1.80 μm-thickness) and film C (2.40 μm-thickness).

Compositional analysis of each film sample was carried out using a Scanning Electron Microscope to which an Energy Dispersive X-ray analyzer (EDX) is coupled (Philips XL 30 FEG). A thin layer of gold (10 nm) was deposited onto the film samples by sputtering to avoid the charging effects of the electron beam accelerated to 20 kV.

It was evaluated the influence of the film thickness on the optical properties as refractive index and optical bandgap and on the chemical composition, as well as the influence of these parameters on photoexpansion and photobleaching phenomena.

2.2. Optical properties

Optical absorption spectra of the films at normal incidence were measured in the 300–1000 nm range using a spectrophotometer model Cary 17 from Varian, and they were used to determine the optical bandgap.

2.3. Photoexpansion and photobleaching experiments

The film samples were covered with a mask and exposed at room temperature to UV radiation (wavelength of 351 nm) of a Kr^+ laser. The laser power density (7.1–70.0 mW/mm^2) and exposure time (30–180 min) were varied. After illumination, the mask was removed from the sample and the exposed area was measured using a profile-meter Formtracer model SV—C525 from Taylor Hobson Precision.

The refractive index of the films was measured at fundamental transverse electric (TE) and magnetic (TM) polarizations with a M-line apparatus model 2010 from Metricon, based on the prismcoupling technique with 0.0005 resolution. A gadolinium garnet (GGG) prism with a refractive index of 1.9644 at 632.8 nm was used. The apparatus was equipped with Si and Ge detectors to collect the visible and NIR (near infrared) light, respectively. He–Ne laser operating at 632.8 nm and one diode laser operating at 1550 nm were employed. The resolution in the determination of the angles, synchronous to the propagation modes, was 0.008°.

In order to observe the shift of absorption edge, which characterizes the photobleaching effect, the absorption spectra of the films were obtained using the Cary 17 spectrophotometer, before and after their exposure to UV light. Once this shift depends on the time of irradiation, the temporal evolution of the beam intensity transmitted through the film was evaluated using a data acquisition system, which is composed of two lock-in amplifiers model SR-530 from Stanford Research Inc. and two silicon detectors.

3. Results and discussion

3.1. Optical bandgap for different films

The optical bandgap is a basic property of optical materials [19]. Band theory for crystalline semiconductors suggests that the absorption coefficient (α) and the energy of the incident photon (E), in the strong absorption region ($\alpha > 10^4\ cm^{-1}$), for allowed direct and indirect transitions, respectively, can be written as [20,21]

$$\alpha E = A_1(E - E_g^1)^{1/2} \quad (1)$$

$$\alpha E = A_2(E - E_g^2)^2 \quad (2)$$

where A_1 and A_2 are two constants, E_g^1 and E_g^2 are direct and indirect bandgaps, respectively. The value of α in term of absorbance can be defined from the relation

$$\alpha = 2.303\left(\frac{A}{d}\right) \quad (3)$$

where A is the optical absorbance and d is the film thickness. The $(\alpha E)^2$ versus the photon energy (E) for the three films A–C are shown in Fig. 1. A linear behavior can be observed in a certain range of the curves, supporting the interpretation of the direct E_g^1 bandgap for thin films [22]. Therefore, E_g^1 of the considered films can be obtained by extrapolating relation (1) between 2.4 and 3.2 eV.

The thickness of each as-prepared film was measured using the profile-meter technique. The thickness values as well as the E_g^1 values for each film are presented in Table 1.

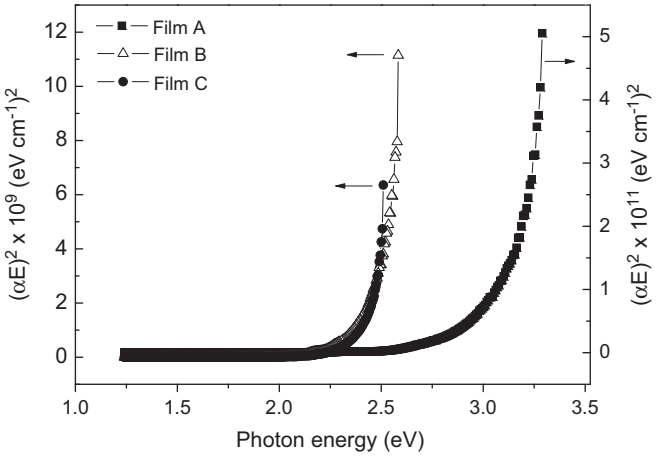

Fig. 1. Determination of optical bandgap energy (E_g^1) by plotting $(\alpha E)^2$ versus incident photon energy (E): the extrapolation of the linear region, in which $(\alpha E)^2$ is equal to zero, corresponds to E_g^1.

Table 1
Optical bandgap (E_g^1) and EDX chemical analysis (at%) for GGSO films with different thicknesses.

Film	Thickness (±0.01 μm)	E_g^1 (±0.05 eV)	At%			
			O (±10%)	S (±5%)	Ga (±5%)	Ge (±5%)
A	0.36	3.21	24	32	1	43
B	1.80	2.52	14	32	1	53
C	2.40	2.49	–	–	–	–

In order to analyze the optical characteristics of the films with regard to the chemical composition, EDX technique was employed. The EDX measurements are listed in Table 1 for films A and B. Clearly, there is a dependence of the bandgap energy with thickness that may be associated to compositional variations. According to literature data [5], E_g^1 shifts to lower energy with the increase of germanium content. For example, E_g^1 of thin GeS_2 films is within 2.3–2.8 eV, while for Ge_2S_3 is 1.75 eV. The fact that bandgap energy, and therefore the absorption coefficient, varies with composition is a difficulty encountered in the characterization of photoinduced effects observed on thin films. The knowledge of the optical properties at the exposure wavelength is crucial for understanding the photoexpansion and photobleaching process. The EDX results of Table 1 show that film A is richer in oxygen than film B, which is richer in Ge. These chemical differences of the films with thickness are associated to an inhomogeneous deposition. Some elements evaporate firstly than other.

3.2. Photoexpansion studies

The films A and B (Table 1) were chosen to study the photoexpansion phenomena as a function of the power density and exposure time. These films were exposed to Kr^+ laser radiation of 351 nm (3.54 eV, this energy is higher than the optical bandgap of these films), using circular hole masks. In Fig. 2 is shown 2D and 3D surface images of the film B after irradiation with power density of 24.3 mW/mm^2 during 2 h. It was observed an expansion with good uniformity on the film surface of around 0.13 μm. The results for film C are not presented, since the dependence with exposure time and power density is similar to the films A and B, as will be presented in Section 3.2.2 of this paper.

After UV irradiation of the films, profile-meter measurements were performed. In the following sections are presented in details the photoexpansion effect as a function of the power density, exposure time and film composition.

3.2.1. Photoexpansion effect versus power density

Fig. 3 illustrates the photoexpansion effect evolution when the exposure time is increased from 30 to 120 min for film A and from 60 to 180 min for film B, using different power density values (7.1–70.0 mW/mm^2).

For the film A, it is noted that the increase of the exposure time results in higher values of photoexpansion for almost all power densities, except at 48 mW/mm^2 for 81 and 120 min (Fig. 3a). A maximum of photoexpansion is observed at around 24.3 mW/mm^2 for all irradiation time. Shorter values of the exposure time imply that the photoexpansion values increase with the power density increase. However, for higher exposure times, the increase of the power density results in lower values of photoexpansion due to the ablation process that may be associated to the fragility of the photoexpanded surface. Fig. 4 shows that the center of the photoexpanded region is thinner than the border. Following a Gaussian profile of the laser beam, the central region receives more photons (energy) than the border and then, the ablation can be more effective.

In the case of the film B, a maximum of photoexpansion is noted, for all irradiation time, using a power density of 24.3 mW/mm^2 (Fig. 3b). The maximum position does not depend on the power density, but the photoexpansion value increases with the exposure time increase. However, increasing the time and the power density, the ablation phenomenon occurs and results in lower values of photoexpansion. Thus, we concluded that the best condition to perform higher photoexpansion values is around 24.3 mW/mm^2 for both films. It seems, for film B, that the photoexpansion effect attains saturation condition at around 180 min.

3.2.2. Photoexpansion effect versus film composition

In order to evaluate the behavior of photoexpansion with film composition, the films A, B and C were illuminated for 2 h with three different power densities: 12.7, 24.3 and 47.2 mW/mm^2 ,respectively. The obtained results for the thickness variation after expansion (Δd) in each film exposed to the three different power

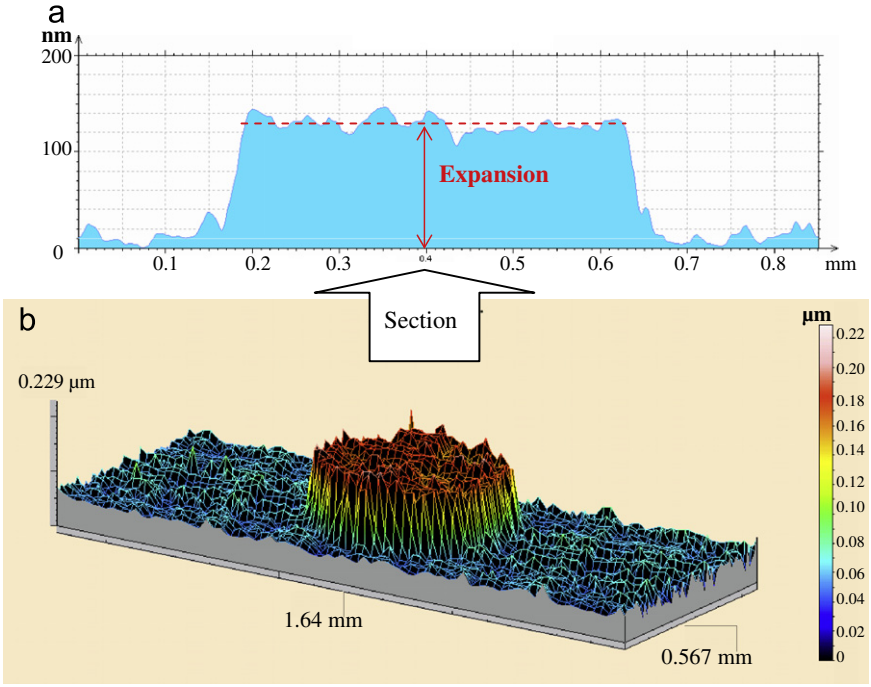

Fig. 2. Confirmation of the occurrence of photoexpansion on a film surface by viewing (a) 2D and (b) 3D surface image of a GGSO film with 1.80 μm-thickness (film B) after UV irradiation exposure to 24.3 mW/mm^2 during 2 h.

densities are presented in Fig. 5. Analyzing the results, one can note that the higher values of expansion are obtained for film A irradiated with a power density of 24.3 mW/mm^2.

In photoexpansion phenomena, the average penetration depth (L) of light is a relevant parameter and depends on the value of the absorption coefficient (α) at the excitation wavelength according to $L=1/\alpha$. It is important to note that films with different compositions exhibit different absorption coefficients. The values obtained for Δd (after illumination with 24.3 mW/mm^2 for 2 h) were compared with L at 351 nm for each film and are listed in Table 2.

The data of Table 2 shows that the film A present a value of Δd greater than L. Good correlation is observed between Δd and L parameters, especially for film B. Since the values of Δd are comparable to the values of L, the photoexpansion effect can be classified as a surface phenomenon.

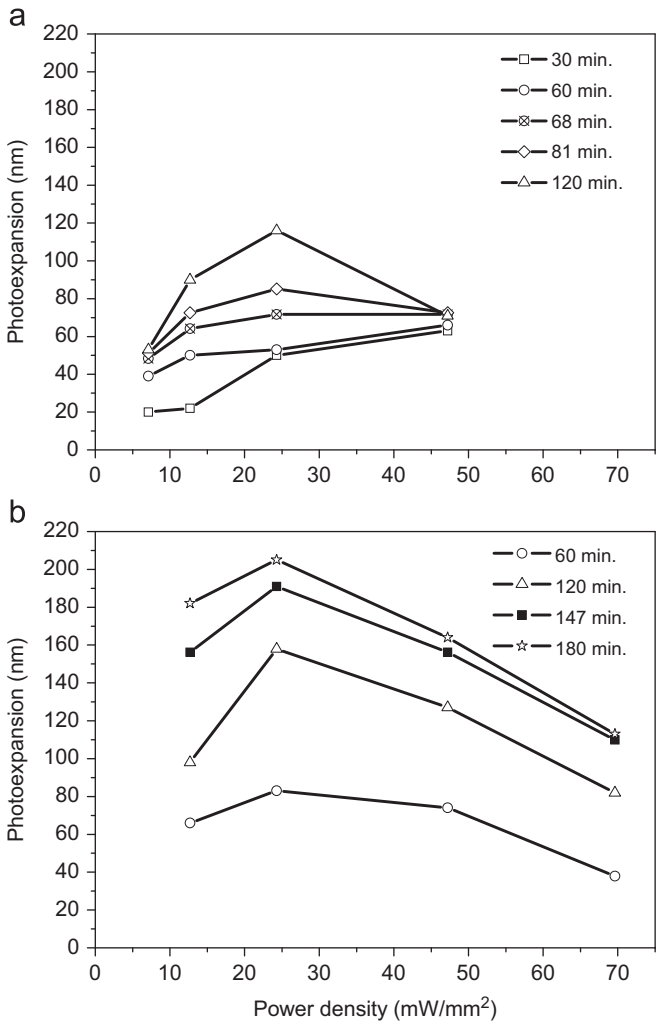

Fig. 3. Photoexpansion effect versus power density. The photoexpansion values as a function of the laser power density with different irradiation time for (a) film A and (b) film B. The lines are used to guide the eyes.

3.3. Photobleaching studies

Not only photoexpansion, but photobleaching phenomenon is also observed when the films are exposed to UV light. This

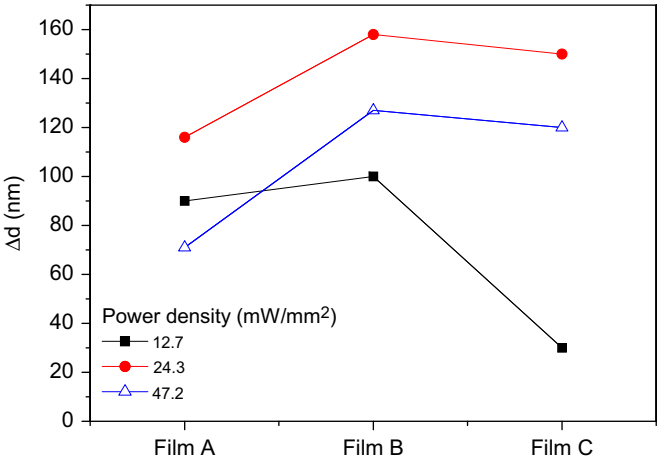

Fig. 5. Photoexpansion values (Δd) for different films: 0.36 μm-Film A, 1.80 μm-film B and 2.40 μm-film C, after exposure to UV light during 2 h with three different power densities.

Table 2
Comparison between thickness variations (Δd) after irradiation and penetration depth of light (L) for films with different thicknesses (d). For each film the fractional expansion ($\Delta d/d$) are also presented.

Film	d ($\pm$0.01 μm)	Δd ($\pm$0.01 μm)	L ($\pm$0.01 μm)
A	0.36	0.12	0.06
B	1.80	0.16	0.16
C	2.40	0.15	0.38

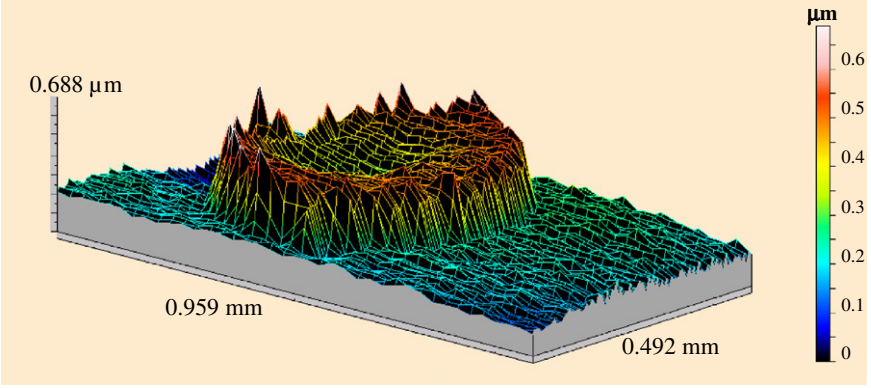

Fig. 4. Ablation process can be seen by the 3D surface image of the film A after UV exposure at 47.2 mW/mm^2 during 2 h. This process may be associated to the fragility of the expanded surface and the Gaussian profile of the laser beam.

photoinduced effect shifts the absorption edge to shorter wavelengths (blue shift). Fig. 6 shows a plot of $(\alpha E)^2$ versus incident photon energy of the film B, before and after illumination with 10.5 mW/mm^2 for 2 h.

In Fig. 6 an increase of the bandgap energy is observed, which is the characteristic of photobleaching. The bandgap energy value as a function of power density is presented in Table 3 for films A and B. The data of this table reveals that the changes in the bandgap values are almost independent of the power density, since the noted differences are within error bar. In fact, the main difference occurs between the non-irradiated samples and those ones exposed to 10.5 mW/mm^2.

Changes in the optical bandgap, as well as photoexpansion, also depend on film composition. This dependence can be analyzed by measurements of saturation time of the photobleaching effect. Variations in the intensity of the beam transmitted through the film were monitored by a data acquisition system. The saturation curves for the films A and B exposed to 24.3 mW/mm^2 are shown in Fig. 7.

The saturation of the effect was observed on films A and B after around 46 min and 133 min (8000 s), respectively. It has been seen previously that there is a dependence of absorption coefficient with film composition and that the photobleaching effect causes a decrease of absorption coefficient, which increases the penetration of light in the material. Since in film A this phenomenon is faster, it is expected that, for a fixed exposure time, this film exhibits photoexpansion values higher than the penetration depth of the incident light. These considerations can be used to explain the results obtained in the characterization of the photoexpansion effect (Table 2).

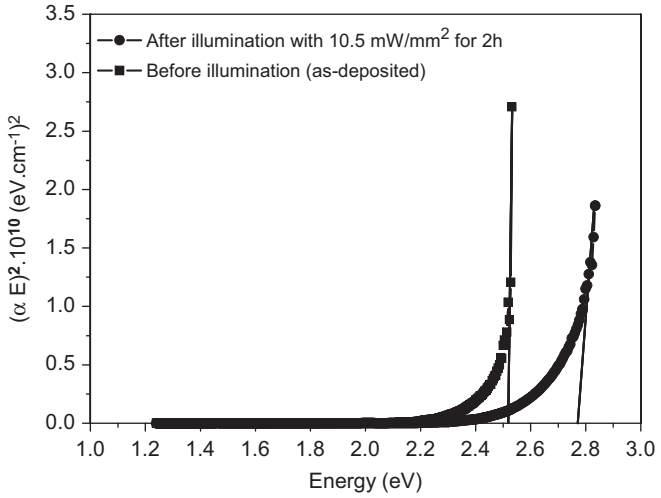

Fig. 6. Plotting of $(\alpha E)^2$ versus incident photon energy (E) for the film B, before and after illumination with 10.5 mW/mm^2 for 2 h, which shows an increase of the optical bandgap, which is characteristic of photobleaching.

Table 3
Optical bandgap (E_g^1) of the films A and B as-prepared and after exposure to UV light with different power densities.

Power density ($\pm \times$ mW/mm^2)	Film A	Film B
	E_g^1 (± 0.05) eV	E_g^1 (± 0.05) eV
Non-irradiated	3.21	2.52
10.5	4.25	2.75
13.6	4.26	2.63
18.2	4.21	2.65

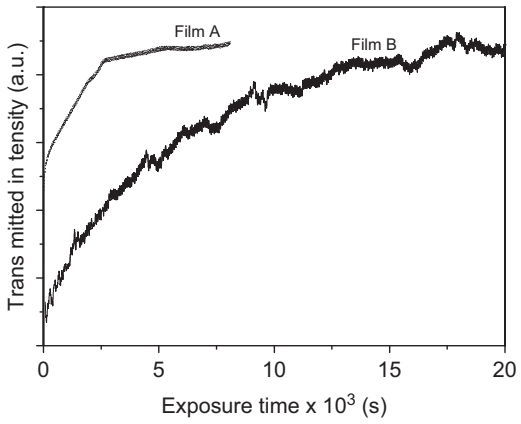

Fig. 7. Saturation curves of the photobleaching effect obtained by *in situ* measurements of the intensity of the transmitted beam through the film with (a) 0.36 μm-thickness: film A and (b) 2.40 μm-thick: film B as a function of irradiation time.

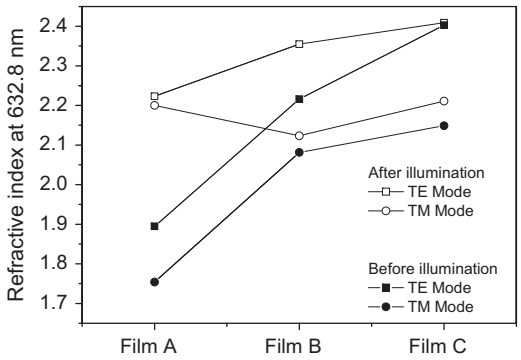

Fig. 8. Effective index of refraction at 632.8 nm for the TE and TM modes of the films before and after illumination with power density of 24.3 mW/mm^2 for each considered film: (0.36 μm-ilm A, 1.80 μm-ilm B and 2.40 μm-ilm C). The lines are used to guide the eyes. The illumination process causes a decrease in refractive index at 632.8 nm and an increase of birefringence.

3.4. Photobleaching effect and refractive index

Refractive index at 632.8 nm was measured for films A–C using the prism-coupling technique. Fig. 8 illustrates the effective index of the fundamental TE and TM modes for each film. The effective index values were measured before and after irradiation with power density of 24.3 mW/mm^2 during 2 h.

One can note that the irradiation process causes a decrease in refractive index at 632.8 nm, which is higher for film A (Δn is approximately 0.32 for the TE mode and 0.45 for the TM mode). As well as in photoexpansion, this behavior can be related to the dependence of the photoinduced effects with exposure time and film composition. Quantitatively, Δn can be calculated by the Lorenz-Lorenz equation [23]:

$$\Delta n = -\frac{(n^2-1)(n^2+2)}{6n^2}\frac{\Delta d}{d} \quad (4)$$

where d is the film thickness and Δd is the increase in thickness after exposure to radiation with above bandgap energy.

Considering the TE results for film A ($d=0.36$ μm, $n=2.2$ and $\Delta n=-0.328$), by Eq. (4), Δd is equal to 0.13 μm. This value is consistent to that obtained by profilometry measurements (0.12 μm) taking into account the same conditions of illumination (Fig. 3a).

The analysis of Fig. 8 with respect to TE mode before irradiation shows that n_{TE} (film A) $<$ nTE (film B) $<$ n_{TE} (film C). However, for TM mode is valid that n_{TM} (film B) $<$ n_{TM} (film C) $<$ n_{TM} (film A).

Comparing the results of before and after illumination, we conclude that the exposure to UV light causes an increase of birefringence ($\Delta n_{TE\text{-}TM}=n_{TE}-n_{TM}$). The $\Delta n_{TE\text{-}TM}$ of film A increased from 0.023 to 0.141 after irradiation. In the case of film C, the $\Delta n_{TE\text{-}TM}$ was equal to 0.198 before illumination and it became 0.254 after illumination. So, the increase in birefringence was more evident for film A, since in this film the photobleaching is faster and the photoexpansion is higher than the penetration depth of the incident light.

Several models have been proposed to explain the considered photoinduced effects. The mechanistic origin behind these effects is not fully understood, but has been interpreted as a consequence of optically induced changes in local bonding configurations. The chemical composition measured by EDX indicated that the irradiated area is oxygen rich. The atomic percentage of this element increased from 24% to 53% for film A and from 14% to 42% for film B [18]. These results are in agreement with the model proposed by Elliott [24], in which the oxygen enters into the film network forming strong covalent bonds with germanium and chalcogen atoms.

4. Conclusions

Photoexpansion and photobleaching effects were observed in amorphous GGSO films when its surface was exposed to UV light (351 nm, 3.54 eV) with energy greater than the bandgap energy. The magnitudes of the expansion and of the absorption edge shift depend on the exposure conditions such as power density and exposure time. Maximum values of photoexpansion were obtained for power density equal to 24.3 mW/mm^2. The composition of the films is also important, since the absorption coefficient also depends on this parameter. Film with less concentration of germanium exhibited faster photobleaching effect and values of photoexpansion higher than the penetration depth of the incident light. In addition, the irradiated GGSO samples exhibited a decrease in refractive index and an increase of birefringence when compared to the non-irradiated samples. EDX measurements indicated that the irradiated area is oxygen richer than the non-irradiated one, suggesting that this element, already incorporated in the glass matrix, has a large participation on the photoinduced phenomena. The film response under laser irradiation leads us to a better knowledge of the oxysulfide photosensibility and allows us project some devices as gratings and waveguides. For this, the knowledge of the refractive and thickness changes with an appropriate power density and exposure time are necessary requirements.

Acknowledgments

Authors are grateful to FAPESP for financial support (05/58396-0). Also, we would like to thank André Luís Romero for his technical assistance.

References

[1] T. Gotoh, K. Tanaka, J. Appl. Phys. 89 (2001) 4697.
[2] M.M. Hafiz, O. El-Shazly, N. Kinawy, Appl. Surf. Sci. 171 (3–4) (2001) 231.
[3] L. Petit, N. Carlie, T. Anderson, J. Choi, M. Richardon, K.C. Richardson, IEEE J. Sel. Top. Quantum Electron. 14 (5) (2008) 1323.
[4] Q. Liu, F. Gan, Mater. Lett. 53 (2002) 411.
[5] K. Tanaka, Y. Kasanuki, A. Odajima, Thin Solid Films 117 (1984) 251.
[6] S.H. Messaddeq, M. Siu, Li, D. Lezal, S.J.L. Ribeiro, Y. Messaddeq, J. Non-Cryst. Solids 284 (2001) 282.
[7] T. Uchino, D.C. Clary, S.R. Elliott, Phys. Rev. Lett. 85 (15) (2000) 3305.
[8] K. Antoine, H. Jain, M. Vlcek, S.D. Senanayake, D.A. Drabold, Phys. Rev. B 79 (2009) 054204.
[9] N. Terakado, K. Tanaka, J. Non-Cryst. Solids 352 (2006) 3815.
[10] Z.H. Zhou, H. Nasu, T. Hashimoto, K. Kamiya, J. Mater. Res 14 (2) (1999) 330.
[11] N. Terakado, K. Tanaka, J. Non-Cryst. Solids 354 (18) (2008) 1992.
[12] K. Tanaka, A. Saitoh, N. Terakado, Photoinduced phenomena in group VIb glasses, J. Mater. Sci.: Mater. Electron 20 (2009) 38.
[13] T. Shimizu, M. Kumeda, I. Watanabe, Y. Nakagaki, Solid State Commun 27 (3) (1978) 223.
[14] K. Shimakawa, A. Kolobov, S.R. Elliot, Adv. Phys 44 (1995) 475.
[15] J.F. Viens, C. Meneghini, A. Villeneuve, T.V. Galstian, E.J. Knystautas, M.A. Duguay, K.A. Richardson, T. Cardinal, J. Lightw. Technol 17 (7) (1999) 1184.
[16] K. Tanaka, N. Toyosawa, H. Hisakuni, Opt. Lett. 20 (19) (1995) 1976.
[17] S.H. Messaddeq, V.R. Mastelaro, M. Siu, Li, M. Tabackniks, D. Lezal, A. Ramos, Y. Messaddeq, Appl. Surf. Sci 205 (2003) 143.
[18] A.C. Mendes, L.J.Q. Maia, S.H. Messaddeq, Y. Messaddeq, A.R. Zanatta, M. Siu Li, Curr. Appl. Phys. 10 (6) (2010) 1411.
[19] E. Kim, Z.T. Jiang, K. No, Jpn. J. Appl. Phys 39 (8) (2000) 4820.
[20] D.L. Wood, J. Tauc, Phys. Rev. B 5 (8) (1972) 3144.
[21] U. Pal, S. Saha, A.K. Chaudhuri, V.V. Rao, H.D. Banerjee, J. Phys. D: Appl. Phys 22 (1989) 965.
[22] U. Pal, D. Samanta, S. Ghorai, A.K. Chaudhuri, J. Appl. Phys. 74 (10) (1993) 6368.
[23] S. Rajagopalan, K.S. Harshavardhan, L.K. Malhotra,, K.L. Chopra, J. Non-Cryst. Solids 50 (1982) 29.
[24] S.R. Elliott, J. Non-Cryst. Solids 81 (1986) 71.